

ARTICLE OPEN



Entanglement-based quantum communication complexity beyond Bell nonlocality

Joseph Ho¹, George Moreno², Samurá Brito², Francesco Graffitti¹, Christopher L. Morrison¹, Ranieri Nery², Alexander Pickston¹, Massimiliano Proietti¹, Rafael Rabelo³, Alessandro Fedrizzi¹ and Rafael Chaves^{2,4}✉

Efficient distributed computing offers a scalable strategy for solving resource-demanding tasks, such as parallel computation and circuit optimisation. Crucially, the communication overhead introduced by the allotment process should be minimised—a key motivation behind the communication complexity problem (CCP). Quantum resources are well-suited to this task, offering clear strategies that can outperform classical counterparts. Furthermore, the connection between quantum CCPs and non-locality provides an information-theoretic insight into fundamental quantum mechanics. Here we connect quantum CCPs with a generalised non-locality framework—beyond Bell’s paradigmatic theorem—by incorporating the underlying causal structure, which governs the distributed task, into a so-called non-local hidden-variable model. We prove that a new class of communication complexity tasks can be associated with Bell-like inequalities, whose violation is both necessary and sufficient for a quantum gain. We experimentally implement a multipartite CCP akin to the guess-your-neighbour-input scenario, and demonstrate a quantum advantage when multipartite Greenberger-Horne-Zeilinger (GHZ) states are shared among three users.

npj Quantum Information (2022)8:13 | <https://doi.org/10.1038/s41534-022-00520-8>

INTRODUCTION

Quantum technology enables applications ranging from fundamentally secure cryptography¹ to quantum teleportation^{2,3} and ultimately the quantum internet as enabled by the distribution of global-scale entanglement resources^{4–6}. Quantum correlations, created in quantum networks, can be harnessed to enhance the efficiency of distributed information processing, i.e. by reducing communication cost; this is exemplified in the use of shared entanglement in communication complexity problems (CCPs)^{7–9}. This will be of interest in near-term quantum computing platforms where many medium-sized nodes are linked to scale up the computational capabilities^{10,11}, where CCP will naturally reside.

Distributed computing represents a highly versatile method of solving demanding tasks by taking a global target function and splitting the input among multiple users. The users act on their inputs locally to solve a global problem with some communication allowed between each of the users. CCP provides the necessary framework in evaluating the ultimate performance of these architectures, notably evaluating the minimum communication overhead needed to achieve the task^{12–14}. Recent developments of CCPs have adopted the use of non-classical resources⁷, and an updated definition for evaluating the complexity of a problem. One might also be interested in obtaining the highest probability of successfully evaluating the target function, with a fixed amount of communication^{8,15–19}. In spite of Holevo’s theorem²⁰—showing that quantum states cannot reduce the cost of transmitting a classical message—if our aim is to compute a function of it, as in the classic CCP setting, quantum resources such as entanglement can demonstrate an improvement. Proof-of-principle experiments have been realised using photonic Bell states²¹, GHZ states²², and entanglement of high-dimensional systems^{23,24}.

We remark that while in this work we focus on entanglement-based CCPs, there is a class of protocols in which the quantum

improvement is obtained not via entanglement but from prepare-and-measure type schemes^{25–28}. Notable experiments of this kind include the quantum fingerprinting protocols^{29,30} and multi-user encoding on non-classical states of light^{13,14,31}. For a broad review of the topic, which includes a discussion of the resources underpinning the quantum advantages in CCPs, see ref. ⁸. More recently, the combination of both entanglement and quantum communication has also started to be considered^{32–34}. Remarkably, it has been proven that quantum advantages in CCPs can be mapped to the violation of Bell inequalities^{19,35,36}, thus establishing an important link between two key concepts of computer science and quantum theory. Moreover, it is widely believed that communication complexity should scale with the size of the input data. Interestingly, this non-triviality of a CCP can be seen as an informational principle for why Nature cannot be more non-local than what is achievable within quantum theory^{37–39}.

The connection between Bell inequalities and communication complexity has only been proven for the standard notion of Bell non-locality, which contrasts quantum mechanics with local hidden-variable (LHV) models. In this standard scenario, one considers a number of separate parties who share a common source of correlations but cannot communicate—an arrangement that is severely limiting, particularly in the context of CCPs. The study of Bell non-locality has, however, produced much more general and stronger notions of non-locality^{40–44}; these include scenarios that allow subsets of parties involved in a Bell experiment to communicate, while the classical description now considers non-local hidden-variable (NLHV) models. So far the connection between CCPs and this generalised Bell non-locality has not been investigated. That is precisely our aim.

Here we show that NLHV models define a new and more general class of CCPs. As opposed to the standard scenario, where each party has an exclusive part of the input data required to compute

¹Institute of Photonics and Quantum Sciences, School of Engineering and Physical Sciences, Heriot-Watt University, Edinburgh EH14 4AS, UK. ²International Institute of Physics, Federal University of Rio Grande do Norte, 59070-405 Natal, Brazil. ³Instituto de Física “Gleb Wataghin”, Universidade Estadual de Campinas, 13083-859 Campinas, Brazil. ⁴School of Science and Technology, Federal University of Rio Grande do Norte, 59078-970 Natal, Brazil. ✉email: rafael.chaves@ufrn.br

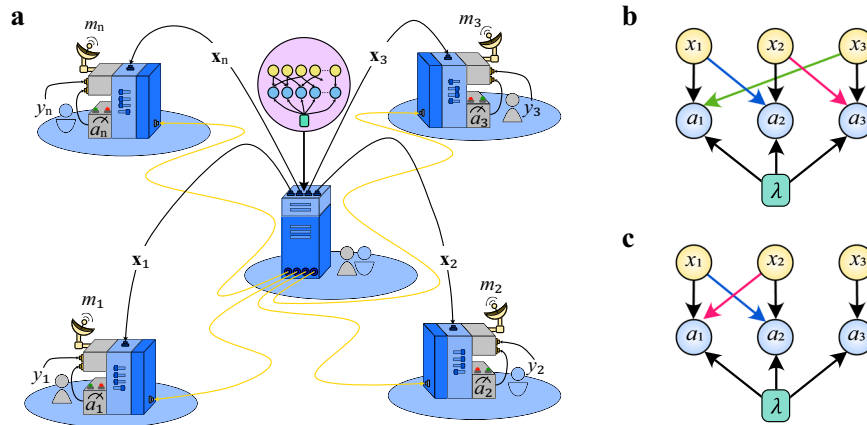


Fig. 1 Distributed computation in a CCP scenario. **a** A central agent allocates resources among a network of n users who independently produce outcomes to solve a collective task. Each user i receives y_i and a subset \mathbf{x}_i of the variables $\{x_1, \dots, x_n\}$ according to some underlying causal structure indicated by the shaded pink region. Each user processes their input data along with shared correlations and broadcast a one-bit message m_i to all others before they compute a function $f(x_1, \dots, x_n, y_1, \dots, y_n)$. When allowing for quantum resources, shared quantum correlations that violate a Bell-like inequality bounding the corresponding NLHV model provide an advantage in the probability of success of the task over its classical counterpart. **b** Causal structure of the three-party GYNI scenario^{41,49} experimentally investigated. The input of each party x_i is communicated to its neighbour to the right (or alternatively, to the left). The variable λ stands for pre-shared (classical) correlations shared among the parties and used to produce respective outcomes, a_i . **c** Causal structure of Svetlichny's scenario⁴⁰ as discussed in Supplementary Methods.

the desired function, in the generalised case the input data can be distributed in arbitrary manners. Every NLHV model defines a specific pattern in which the input data is distributed among the parties, see Fig. 1a. Moreover, every full correlator Bell inequality bounding the classical correlations in such NLHV models not only defines a target function in the CCP but also the corresponding probability of success in trying to compute it with a restricted amount of communication between the parties. Thus, the violation of these Bell inequalities is a necessary and sufficient condition for a quantum advantage in generalised CCPs. This establishes the general connection between this form of nonclassicality emerging from NLHV models and a relevant quantum information task. We experimentally investigate a three-party CCP task with a causal structure inspired by the guess-your-neighbour-input (GYNI) non-local game, and demonstrate an increased winning probability when using quantum resources that violate the associated Bell-like inequality. This exemplifies the need to consider the underlying causal structures when defining the Bell-like inequalities for generalised CCPs.

RESULTS

Bell scenarios with non-local hidden-variable models

In a standard Bell scenario, each of n distant parties receives an input x_i and produces an output a_i (with $i = 1, \dots, n$). A local hidden-variable description implies that the observed probability distribution $p(a_1, \dots, a_n | x_1, \dots, x_n) = p(\mathbf{a} | \mathbf{x})$ can be decomposed as

$$p(\mathbf{a} | \mathbf{x}) = \sum_{\lambda} p(a_1 | x_1, \lambda) \dots p(a_n | x_n, \lambda) p(\lambda), \quad (1)$$

where λ is a classical random variable accounting for all correlations observed between the measurement outcomes of the distant parties. In turn, in a quantum description, Born's rule implies that

$$p(\mathbf{a} | \mathbf{x}) = \text{Tr} \left[\left(M_{a_1}^{x_1} \otimes \dots \otimes M_{a_n}^{x_n} \right) \rho \right], \quad (2)$$

where $M_{a_i}^{x_i}$ are measurement operators and ρ describes the quantum state shared between the parties. As shown by Bell⁴⁵, there are quantum correlations (2) that cannot be written as (1). This is the phenomenon known as Bell non-locality and is

witnessed by the violation of Bell inequalities^{35,45}, where linear constraints on the probabilities should be respected by any distribution of the form (1).

In spite of its importance, the usual Bell scenario is rather restrictive, in that no communication can take place between the parties. Alternatively, one can think of an external agent that generates a sequence of values of n random variables $\{x_i\}$ and sends (possibly overlapping) subsets of this sequence to each of the n parties involved in the Bell test. In this more general scenario the i th party can receive a total of l_i inputs that we label as $x_{i,j} \in \{x_i\}$ with $j = 1, \dots, l_i$ and $x_{i,1} = x_i$. Let the set of inputs of party i be organised in a vector $\mathbf{x}_i = \{x_{i,j} | j = 1, \dots, l_i\}$. A classical description is then given by a NLHV model

$$p(\mathbf{a} | \mathbf{x}) = \sum_{\lambda} p(a_1 | \mathbf{x}_1, \lambda) \dots p(a_n | \mathbf{x}_n, \lambda) p(\lambda), \quad (3)$$

that can be graphically represented by a directed acyclic graph where each measurement outcome a_i has a set of parents $x_{i,j}$. See Fig. 1b and Fig. 1c for examples.

Analogously to Eq. (2), the set of quantum correlations in this extended Bell scenario is described as

$$p(\mathbf{a} | \mathbf{x}) = \text{Tr} \left[\left(M_{a_1}^{x_1} \otimes \dots \otimes M_{a_n}^{x_n} \right) \rho \right], \quad (4)$$

that is, the measurement settings of each party may now depend on subsets of $\{x_i\}$ and might have an overlap for different parties. From a broad perspective, we are imposing a given causal structure to the experiment, one in which parts of the input of a given party can also be known by other distant parties. Similarly to the usual Bell's theorem, we will be interested in whether: (i) there are quantum correlations, Eq. (4), that do not have a classical description as in Eq. (3); and (ii) this nonclassicality can be harnessed in the processing of information, in particular in CCPs.

The answer to the first question will inherently depend on the specific causal structure under analysis but positive examples are known^{40–44,46–48} and will be explored in more detail below. Preceding this, a general answer to the second question is the central theoretical result of this paper.

Communication complexity and Bell inequalities

Without loss of generality, in a usual CCP involving n participants¹⁶, each party i receives two bits— x_i and y_i —and can broadcast to all other parties just a one-bit message. As an example of such a CCP, one can consider that the parties want to schedule an appointment, their local inputs represent their availability in different time slots and thus the function they want to compute relates to finding a time slot when all of them are available. However, one can think of more general scenarios where the schedule (or part of it) from one of the participants is known to the others. Having this in mind in our generalised CCP each party i has access to the random variables $\mathbf{x}_i = \{x_{ij} | j = 1, \dots, l_i\} \subset \{x_i | i = 1, \dots, n\}$ and y_i , where $x_i, y_i \in \{\pm 1\}$ (see Fig. 1a). The values of the variables x_i are drawn from a joint probability distribution $q(x_1, \dots, x_n)$, while the y_i 's are independently drawn from a uniform distribution. Furthermore, the parties are also allowed to share correlated systems and use their measurement outcomes $a_i \in \{\pm 1\}$ in the execution of the protocol. Here, we follow closely the conceptual framework of the seminal results in ref.¹⁶, which provides a general connection between LHV models and CCPs. As in ref.¹⁶, the goal is for each party to evaluate a binary function $f(x_1, \dots, x_n, y_1, \dots, y_n) = f(\mathbf{x}, \mathbf{y}) = f$ given by

$$f(\mathbf{x}, \mathbf{y}) = y_1 \dots y_n S[Q(x_1, \dots, x_n)], \quad (5)$$

where $Q = Q(x_1, \dots, x_n)$ is a function of all inputs, and $S[Q] = \frac{Q}{|Q|}$ is the sign function, with the restriction that each party i can only broadcast a single bit $m_i = m_i(x_{i,1}, \dots, x_{i,l_i}, y_i, a_i)$ to every other party j . If party i guesses $G_i(\mathbf{x}, \mathbf{y})$ for the function $f(\mathbf{x}, \mathbf{y})$, its probability of success is given by

$$\mathcal{P}_i = \frac{1}{2^n} \sum_{\substack{x_1, \dots, x_n \\ y_1, \dots, y_n}} q(\mathbf{x}) P(G_i(\mathbf{x}, \mathbf{y}) = f(\mathbf{x}, \mathbf{y})), \quad (6)$$

where $P(G_i(\mathbf{x}, \mathbf{y}) = f(\mathbf{x}, \mathbf{y})) = 1$ if $G_i(\mathbf{x}, \mathbf{y}) = f(\mathbf{x}, \mathbf{y})$ and 0 otherwise.

Consider now a general Bell inequality of the form

$$B_n = \sum_{x_1, \dots, x_n = -1}^1 Q(x_1, \dots, x_n) E_{x_1, \dots, x_n} \leq B_n^C, \quad (7)$$

where $Q(x_1, \dots, x_n)$ is the coefficient of E_{x_1, \dots, x_n} , which stands for the full correlation function

$$E_{x_1, \dots, x_n} = P_{x_1, \dots, x_n} \left(\prod_{i=1}^n a_i = 1 \right) - P_{x_1, \dots, x_n} \left(\prod_{i=1}^n a_i = -1 \right), \quad (8)$$

and B_n^C is the classical bound associated with a given causal structure described by the NLHV decomposition in Eq. (3). Then, our main theoretical result is to show that a violation of such a Bell inequality is necessary and sufficient to lead to a quantum advantage in a CCP related to the computation of the function in Eq. (5). This is stated in the following theorem, the proof of which is elaborated in the Methods and Supplementary Methods.

Theorem 1. Given a Bell inequality of the form (7), the optimal classical probability of success \mathcal{P}_i^C of party i computing the function

$$f(\mathbf{x}, \mathbf{y}) = y_1 \dots y_n S[Q(x_1, \dots, x_n)], \quad (9)$$

is limited by

$$\mathcal{P}_i^C \leq \frac{1}{2} + \frac{B_n^C}{2\Gamma}, \quad \forall i; \quad (10)$$

with $\Gamma = \sum_{x_1, \dots, x_n = -1}^1 |Q(x_1, \dots, x_n)|$. Moreover, using the correlations shared between the parties there is a protocol achieving

$$\mathcal{P}_i = \frac{1}{2} + \frac{B_n}{2\Gamma}, \quad \forall i; \quad (11)$$

thus showing that a violation of the Bell inequality (7) is both necessary and sufficient for an advantage in the CCP.

This result shows that every full correlator Bell inequality that displays a quantum violation is associated with a CCP with quantum advantage, even in scenarios where the parties can communicate. As detailed in the Methods and Supplementary Method, to achieve the probability of success (11) we provide a protocol, which we prove to be optimal for classical and quantum systems, in which the message m_i communicated from one party to all others has the form $m_i = y_i a_i$, that is, the product of its input y_i with the measurement outcome a_i . Interestingly, as we show next, there are inequalities that do not show quantum violations in standard Bell scenarios, that, however, is violated if such communication is allowed. In order to illustrate the theorem, we present a Bell inequality along with its corresponding CCP, associated with a tripartite Bell scenario with communication-related to the *guess-your-neighbour's-input* (GYNI) scenario⁴⁹. We then proceed to implement this scenario experimentally. As a second illustration of the Theorem, we introduce the 'Svetlichny' scenario⁴⁰ in the Supplementary Methods.

Guess-your-neighbour's-input scenario

The causal structure for this scenario (see Fig. 1b), akin to the guess-your-neighbour's-input game⁴⁹, was introduced in ref.⁴¹, leading to a new type of multipartite non-locality. Classical correlations (3) are bounded by the inequality⁴¹

$$B_G = \sum_{x_1, x_2, x_3 = -1}^1 Q_G(x_1, x_2, x_3) E_{x_1, x_2, x_3} \leq B_G^C, \quad (12)$$

with $B_G^C = 6$ and $Q_G(x_1, x_2, x_3) = 1 - \frac{(1-x_1)(1-x_2)(1-x_3)}{4}$. Following the causal structure in Fig. 1b and general prescription of the CCP, party 1 broadcasts a bit $m_1(x_1, x_3, y_1, a_1)$, party 2, $m_2(x_1, x_2, y_2, a_2)$, and party 3, $m_3(x_2, x_3, y_3, a_3)$.

According to the Theorem, the classical probability of success in computing the associated function is $P_{Suc}^C \leq 7/8 = 0.875$. As shown in ref.⁴¹, a quantum violation of this inequality is not possible if party i only has access to the input x_i . If, however, the three parties share a GHZ state of the form $|\text{GHZ}\rangle = (|000\rangle + |111\rangle)/\sqrt{2}$, and are able to choose their measurements according to the GYNI causal structure depicted in Fig. 1b, the inequality (12) can be violated up to $B_G \approx 7.39$. This results in a higher probability of success, $P_{Suc} \approx 0.962$, a quantum advantage in this CCP. As shown in the Supplementary Methods, resorting to a generalisation of the NPA hierarchy⁵⁰ (a secondary but still relevant technical contribution of our results), this is the optimal quantum value.

Experimental implementation

We experimentally investigate the GYNI scenario by producing a tripartite GHZ state encoded in the polarisation of telecom-wavelength photons (see Fig. 2). We measure the correlation terms defined by inequality (12) to demonstrate that the experimentally observed state can violate the inequality, which is both necessary and sufficient for a quantum advantage in the CCP. For each correlation term, we implement the optimal measurement settings in Alice, Bob and Charlie's polarisation analysers and record the photon statistics for all 2^3 outcomes to evaluate the expectation values as shown in Fig. 3. See Methods for details on the optimal measurement settings. From our measurements we obtain a correlation value of $B_G = 7.023 \pm 0.036$, representing a violation of the inequality (12) by 28 standard deviations with respect to the classical bound of $B_G^C = 6$. Using Eq. (11), the observed violation translates to a probability of correctly computing the CCP in this GYNI scenario of $P_{Suc} = 0.9389 \pm 0.0049$.

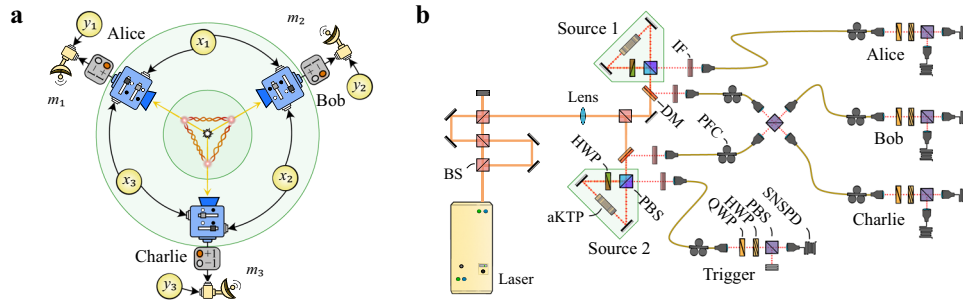


Fig. 2 Experimental layout. **a** Conceptual layout of the three-user GYNI protocol. The tripartite GHZ state is distributed among the three users who locally measure their photon based on input bits $\{x_i, x_j\}$. To compute the target function, each user broadcasts a one-bit message using their measured outcome and a local bit, y_i . **b** We create the GHZ state using two polarisation-entangled photon-pair sources and a linear-optics fusion gate. Each source is implemented with an aperiodically poled KTP crystal embedded in a Sagnac loop that is optically pumped bidirectionally using a picosecond mode-locked laser, see Methods for details. Down-converted photons are separated from the pump laser using dichroic mirrors (DM) and interference filters (IF) then fibre coupled into single mode fibres. One photon from each source non-classically interferes on a polarising beamsplitter (PBS) creating the three-photon GHZ state conditioned on measuring the fourth photon as a Trigger. Each user performs projective measurements on their qubit using a quarter-wave plate (QWP), half-wave plate (HWP), and PBS. Single photons are detected using superconducting nanowire single-photon detectors (SNSPD) and time-tagged for coincidence measurements within a 1 ns window.

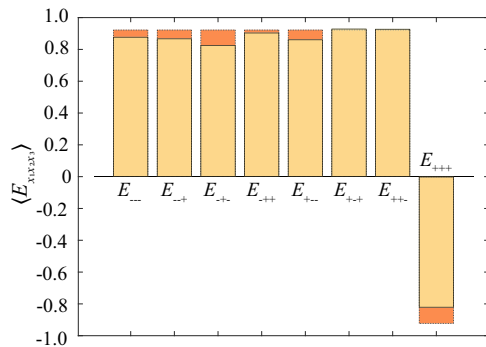


Fig. 3 Experimental results. Experimentally measured correlation terms belonging to the non-local Bell inequality in the GYNI scenario, $E_{x_1 x_2 x_3}$ where $\{x_1, x_2, x_3\} \in \{\pm 1\}$. Orange bars represent the theoretical values assuming the optimal measurement settings while yellow bars show the experimentally observed values. We evaluate the inequality and report a correlation value of $B_G = 7.023 \pm 0.036$. Errors as estimated by Monte Carlo sampling, using $N = 200$ runs and assuming Poissonian statistics, are omitted as they are too small to be visible.

We implement the tripartite GYNI protocol in a faithful round-by-round execution to verify the general connection between CCPs and NLHV models established in this work. In each round of the protocol, we distribute a GHZ state to three users, and use the NIST randomness beacon⁵¹ to generate randomised input data $(x_1, x_2, x_3, y_1, y_2, y_3)$. Each user receives their input bits $\{x_i, x_j, y_i, y_j\}$, updates their polarisation analysers with their respective measurement settings $M^{(x_i, x_j)}$. Since the generation of the GHZ state is non-deterministic, we post-select on the first four-fold detection coincidence event for each round. This heralds successful distribution of the resource state and enables us to record the outcome a_i of each player—see Methods for details. Finally, every user announces their one-bit message, $m_i = y_i \cdot a_i$, evaluates a guess for the round and compares the joint result with the value of the target function, $f(\mathbf{x}, \mathbf{y}) = y_1 y_2 y_3 \left(1 - \frac{(1-x_1)(1-x_2)(1-x_3)}{4} \right)$, obtaining a pass/fail for the round.

We perform the protocol for a total of 10,100 rounds and observe successful outcomes for 9403 rounds, corresponding to a probability of success of $P_{Suc} = 0.9310$. The experimentally measured probability of success is slightly smaller than the

estimated value obtained by the measured violation of the inequality. This is likely due to drifts in the setup when performing the protocol over a large number of rounds. For the round-by-round execution we collected 2 days worth of statistics, whilst the measurements pertaining to the inequality violation were recorded in less than an hour. One of the main limitations in our measurement rate is the use of motorised stages for rotating the waveplates. As a result the majority of the data acquisition time is currently due to the time needed to update the measurement settings. Our implementation of the protocol obtained a probability of success beyond what is achievable when parties only have access to classical shared resources, i.e. $P_{Suc}^C \leq 0.875$, unambiguously demonstrating the quantum advantage as it was defined in ref.¹⁶.

DISCUSSION

Generalisations of Bell's theorem to more complex causal networks and in particular those involving communication between the parties are attracting growing attention. On one side they unveil new^{48,52} and sometimes stronger^{40,42} kinds of quantum non-locality. On the other hand, the practical use of this nonclassicality in the processing of information has so far been limited to specific cases, such as device-independent entanglement quantification⁵³, closing attacks in multipartite cryptographic protocols⁵⁴, and game theory⁵⁵. Here we proposed a general approach by showing that non-local hidden-variable models introduce a new class of communication complexity problems that contain previous versions¹⁶ as special cases. The Bell inequalities bounding classical correlations in such models can be mapped to the functions to be computed in the associated communication problem. Further, the violations of these inequalities provide a necessary and sufficient condition for a quantum advantage over the best possible classical protocol. Our results are theoretically proven in full generality and validated for a specific scenario in an experiment based on a high-fidelity tripartite GHZ state, demonstrating a quantum violation of the Bell inequality (12), akin to the guess-your-neighbour-input scenario^{41,49}.

Our implementation of the protocol in its entirety—using randomised measurement settings on a round-by-round basis—demonstrates the advantage in a CCP task when using non-locality as a quantum resource. Future quantum networks will enable the implementation of increasingly sophisticated CCP related tasks over distances, e.g. linking a cluster of network

nodes. Here the entanglement resources are produced in the telecom regime, enabling low-loss transmission in optical fibres connecting network nodes. Additionally, the investigation of different CCP tasks associated with “network-friendly” multipartite entangled states such as graph states would further provide utility in more generalised scenarios.

In spite of the generality of our results a few relevant questions still require further in-depth analysis. As we show here, the violation of a full correlator Bell inequality is a necessary and sufficient condition for a quantum advantage, even in NLHV models related to Bell scenarios with communication. But for which NLHV models are such violations possible? Initial attempts⁴¹ have provided partial answers in the case where the quantum correlations are non-signalling, that is, the quantum measurements do not make use of the inputs of other parties. The answer to the more general case remains open. Further, we have focused here on full correlator Bell inequalities and it is known that, in the more general case, the violation of Bell inequalities does not necessarily lead to quantum improvements in standard CCPs⁵⁶. In view of that, analysing under which conditions quantum advantages in generalised CCPs can also be connected with Bell inequalities involving marginals and more measurement outcomes is an interesting question for future research.

METHODS

Entangled photon source

We employ two parametric down-conversion (PDC) sources to create the polarisation-encoded GHZ state. Each source consists of a 30 mm aperiodically poled KTP (aKTP) crystal designed to produce spectrally pure photon pairs at 1550 nm in the Type-II configuration⁵⁷. This is achieved through an optimised domain engineering technique, where aperiodic poling achieves a non-linear Phase Matching Function (PMF) that approximates a Gaussian, resulting in near-optimal bi-photon spectral purity⁵⁸. This approach allows our photon sources to operate without lossy narrowband filters—the interference filters have nominal full-width-half-maximum bandwidth of 8.8 nm—allowing higher heralding and collection efficiencies while maintaining high visibility non-classical interference as required for producing multi-photon states efficiently. Our crystals are designed for matching a transform-limited Sech-shaped pump spectrum with a pulse duration of 1.3 ps. The domain engineered crystal is embedded in a Sagnac loop, which generates polarisation-entanglement between the photon pair. A lens with a 50 cm nominal focal length is used to focus the pump field into each crystal, leading to a source brightness of ~ 2400 pairs $\text{mW}^{-1} \text{s}^{-1}$ and heralding efficiencies of $\sim 60\%$. With 50 mW of pump power we witness interference visibility of $94.2 \pm 1.5\%$ between photons generated from independent sources without any filtering. In addition, the picosecond laser is spatially multiplexed attaining 320 MHz repetition rate. This is implemented using two free-space delay loops using 50:50 beamsplitters (BS) and mirrors. This allows the peak power per pulse to be reduced to lower the probability of unwanted multi-photon events at the same pump power.

One photon from each source interferes non-classically on a PBS such that conditional on measuring one photon in each output detector set; Alice (A), Bob (B), Charlie (C), and Trigger (T), the quantum state of the overall four-photon system is,

$$|\Psi\rangle_{A,B,C,T} = \frac{|HVVH\rangle + e^{i\theta}|VHHV\rangle}{\sqrt{2}}, \quad (13)$$

where $|H\rangle \equiv |0\rangle$ and $|V\rangle \equiv |1\rangle$ in the logical basis encoding⁵⁹. We note the phase shift θ is intrinsic to the optical components in our setup and can be compensated by local operations on any one of the entangled qubits. Our setup uses standard polarisation measurement analysers—which consists of a QWP, HWP, and PBS where the output modes are fibre coupled to SNSPDs—to perform arbitrary projective measurements on each qubit.

To obtain the three-qubit GHZ state for this experiment we project the Trigger photon onto the state, $|\theta\rangle \doteq (|H\rangle + e^{-i\theta}|V\rangle)/\sqrt{2}$, which ensures entanglement among the remaining photons and simultaneously implements the phase correction. Detecting a photon after the PBS projects the

remaining three photons onto the following state,

$$|\Psi\rangle_{A,B,C} = \frac{|HHH\rangle + |VVV\rangle}{\sqrt{2}}, \quad (14)$$

up to a local bit-flip which is implemented in the respective user’s measurement stage with the use of the polarisation fibre controller. We perform quantum state tomography and reconstruct the density matrix to characterise the general properties of the GHZ state. We observe the fidelity to the ideal state to be $\mathcal{F} = 0.9508 \pm 0.0031$ and a state purity of $\mathcal{P} = 0.9255 \pm 0.0058$. Uncertainties are reported for one standard deviation and obtained by Monte Carlo sampling using 200 runs, assuming Poissonian statistics.

Our linear-optics setup produces the multipartite entangled state non-deterministically, with a success probability of $P_{\text{Suc}} = 1/2$. Nonetheless, provided one photon is detected at the measurement stages of Alice, Bob, Charlie, and the Trigger, we obtain the state in (13). Thus, in the round-by-round implementation we post-select on four-fold coincidence events to record an outcome for the round. We implement this using the fast coincidence logic to record only the first valid four-fold event after the polarisation analysers are set. Then, as per the protocol, the next round proceeds by updating the measurement stage settings.

Measurement settings

In our experiment the measurement setting in each round for each user is determined by two input bits $\{x_i, x_j\}$, distributed as per the GYNI scenario. As such, each user has four possible projective measurement settings, $M^{(x_i, x_j)}$, as shown in Table 1.

The correlators, $E_{x_1 x_2 x_3} = \langle A_{x_1 x_3} B_{x_1 x_2} C_{x_2 x_3} \rangle$, measured in our experiment are expressed in conventional notation in which the subscript indices, denote the local variable x_i assigned to each user prior to distribution to their neighbour. As such we make use of Table 2 to determine the measurements that is performed by each user.

Our measurement apparatus allows us to perform arbitrary projective measurements by using the HWP and QWP to rotate the measurement basis. Placement of detectors behind both outputs of the PBS enables us to obtain outcomes spanning the full basis set.

Calculating correlations

In the experiment each user’s measurement stage is accompanied by two detectors to measure both outputs of the PBS. This allows us to directly sample the joint outcomes for a given basis defined by the measurement settings of each user. For example to evaluate the correlator E_{+++} we set the measurement waveplates to implement $M_1^{(+,+)}$, $M_2^{(+,+)}$, and $M_3^{(+,+)}$, for Alice, Bob, and Charlie, respectively. We record the three-fold coincidence events according to the outcome detector patterns and evaluate,

$$E_{+++} = \langle M_1^{(+,+)} M_2^{(+,+)} M_3^{(+,+)} \rangle = \frac{C_{+++} - C_{++-} - C_{+-+} + C_{+--} - C_{-++} + C_{-+-} + C_{-+} - C_{--}}{C_{+++} + C_{++-} + C_{+-+} + C_{+--} + C_{-++} + C_{-+-} + C_{-+} + C_{--}}, \quad (15)$$

where C_{ijk} are the number of coincidences, and indices $\{i, j, k\} \in \{+, -\}$ denote the outcome for Alice, Bob, and Charlie, respectively. Finally, we note that the other correlators are evaluated in the same way following the measurement settings outlined previously.

Sketch of the Theorem’s proof

The full proof of (10) is rather lengthy and presented in the Supplementary Methods. Here we focus on (11). First, notice that full correlators can be

Table 1. Optimal projective measurement settings for each player in three-user GYNI CCP scenario.

| Alice | Bob | Charlie |
|--------------------------------------|--|--|
| $M_1^{(+,+)} = \frac{1+\sigma_x}{2}$ | $M_2^{(+,+)} = \frac{1+\sigma_x}{2}$ | $M_3^{(+,+)} = \frac{1+(-0.38\sigma_x - 0.92\sigma_y)}{2}$ |
| $M_1^{(+,-)} = \frac{1-\sigma_y}{2}$ | $M_2^{(+,-)} = \frac{1}{2} + \frac{-\sigma_x + \sigma_y}{2\sqrt{2}}$ | $M_3^{(+,-)} = \frac{1+(-0.92\sigma_x - 0.38\sigma_y)}{2}$ |
| $M_1^{(-,+)} = \frac{1+\sigma_x}{2}$ | $M_2^{(-,+)} = \frac{1+\sigma_y}{2}$ | $M_3^{(-,+)} = \frac{1+(-0.38\sigma_x + 0.92\sigma_y)}{2}$ |
| $M_1^{(-,-)} = \frac{1+\sigma_y}{2}$ | $M_2^{(-,-)} = \frac{1}{2} + \frac{-\sigma_x + \sigma_y}{2\sqrt{2}}$ | $M_3^{(-,-)} = \frac{1+(0.92\sigma_x - 0.38\sigma_y)}{2}$ |

Table 2. Measurement settings for measurements of each correlator term in the three-user GYNI inequality.

| Measurement setting | Alice | Bob | Charlie |
|---------------------|---------------|---------------|---------------|
| E_{+++} | $M_1^{(+,+)}$ | $M_2^{(+,+)}$ | $M_3^{(+,+)}$ |
| E_{++-} | $M_1^{(+,-)}$ | $M_2^{(-,+)}$ | $M_3^{(-,+)}$ |
| E_{+-+} | $M_1^{(+,+)}$ | $M_2^{(+,-)}$ | $M_3^{(+,-)}$ |
| E_{+--} | $M_1^{(+,-)}$ | $M_2^{(-,-)}$ | $M_3^{(-,-)}$ |
| E_{-++} | $M_1^{(-,+)}$ | $M_2^{(+,+)}$ | $M_3^{(+,+)}$ |
| E_{-+-} | $M_1^{(-,-)}$ | $M_2^{(-,+)}$ | $M_3^{(-,+)}$ |
| E_{--+} | $M_1^{(-,+)}$ | $M_2^{(+,-)}$ | $M_3^{(+,-)}$ |
| E_{---} | $M_1^{(-,-)}$ | $M_2^{(-,-)}$ | $M_3^{(-,-)}$ |

written as

$$E(x_1, \dots, x_n) = S[Q] \left[2P_{x_1, \dots, x_n} \left(\prod_{i=1}^n a_i = S[Q] \right) - 1 \right]. \quad (16)$$

Inequality (7) can then be rewritten as

$$\sum_{x_1, \dots, x_n = -1}^1 q^*(x_1, \dots, x_n) \times P_{x_1, \dots, x_n} \left(\prod_{i=1}^n a_i = S[Q(x_1, \dots, x_n)] \right) \leq \frac{1}{2} + \frac{B_n}{2\Gamma}. \quad (17)$$

in which $q^*(x_1, \dots, x_n) = \frac{|Q(x_1, \dots, x_n)|}{\Gamma}$. In what follows we will set $q(x_1, \dots, x_n) = q^*(x_1, \dots, x_n)$, thus connecting the probability distribution $q(x_1, \dots, x_n)$ governing the variables x_1, \dots, x_n with the coefficients $Q(x_1, \dots, x_n)$ defining the Bell inequality (7).

The protocol proceeds as follows. Each party i chooses a measurement to perform from the set $\{x_{ij} | j = 1, \dots, l_i\}$, obtaining outcome a_i . Each party, then, broadcasts to all other parties the message $m_i = a_i y_i \in \{\pm 1\}$. In the final step all parties make the same guess about the function f to be computed, given by

$$G_i = \prod_{j=1}^n m_j = y_1 \dots y_n a_1 \dots a_n, \quad \forall i. \quad (18)$$

A comparison between the guess of each party (18) and the function (5) to be computed shows that, given a sequence of inputs $x_1, \dots, x_n, y_1, \dots, y_n$, the success probability is independent of y_1, \dots, y_n and given by $P_{x_1, \dots, x_n} \left(\prod_{i=1}^n a_i = S[Q(x_1, \dots, x_n)] \right)$. Hence, since the variables x_1, \dots, x_n are sorted according to a distribution $q(x_1, \dots, x_n)$ and variables y_1, \dots, y_n are uniformly sorted, the final probability of success is

$$P_{Suc} = \sum_{x_1, \dots, x_n = -1}^1 q(x_1, \dots, x_n) \times P_{x_1, \dots, x_n} \left(\prod_{i=1}^n a_i = S[Q(x_1, \dots, x_n)] \right).$$

A comparison with (17) leads directly to (11).

DATA AVAILABILITY

The data supporting the findings of this work are available from the corresponding author upon reasonable request.

Received: 11 June 2021; Accepted: 3 December 2021;

Published online: 03 February 2022

REFERENCES

- Gisin, N., Ribordy, G., Tittel, W. & Zbinden, H. Quantum cryptography. *Rev. Mod. Phys.* **74**, 145 (2002).
- Bennett, C. H. et al. Teleporting an unknown quantum state via dual classical and einstein-podolsky-rosen channels. *Phys. Rev. Lett.* **70**, 1895 (1993).
- Ren, J.-G. et al. Ground-to-satellite quantum teleportation. *Nature* **549**, 70 (2017).
- Kimble, H. J. The quantum internet. *Nature* **453**, 1023 (2008).
- Wehner, S., Elkouss, D. & Hanson, R. Quantum internet: a vision for the road ahead. *Science* **362**, eaam9288 (2018).
- Brito, S., Canabarro, A., Chaves, R. & Cavalcanti, D. Statistical properties of the quantum internet. *Phys. Rev. Lett.* **124**, 210501 (2020).
- Cleve, R. & Buhrman, H. Substituting quantum entanglement for communication. *Phys. Rev. A* **56**, 1201 (1997).
- Buhrman, H., Cleve, R., Massar, S. & de Wolf, R. Nonlocality and communication complexity. *Rev. Mod. Phys.* **82**, 665 (2010).
- Brukner, C., Żukowski, M. & Zeilinger, A. Quantum communication complexity protocol with two entangled qutrits. *Phys. Rev. Lett.* **89**, 197901 (2002).
- Buhrman, H. & Röhrig, H. In *Mathematical Foundations of Computer Science 2003*, 1–20 (eds. Rovan, B. & Vojtáš, P.) (Springer Berlin Heidelberg, 2003).
- Beals, R. et al. Efficient distributed quantum computing. *Proc. R. Soc. Lond. A* **469**, 20120686 (2013).
- Yao, A. C.-C. Some complexity questions related to distributive computing (preliminary report). In *Proc. eleventh annual ACM symposium on Theory of computing*, 209–213 (Association for Computing Machinery, 1979).
- Trojek, P. et al. Experimental quantum communication complexity. *Phys. Rev. A* **72**, 050305 (2005).
- Kumar, N., Kerenidis, I. & Diamanti, E. Experimental demonstration of quantum advantage for one-way communication complexity surpassing best-known classical protocol. *Nat. Commun.* **10**, 4152 (2019).
- Buhrman, H., Cleve, R. & Van Dam, W. Quantum entanglement and communication complexity. *SIAM J. Comput.* **30**, 1829 (2001).
- Brukner, C., Żukowski, M., Pan, J.-W. & Zeilinger, A. Bell's inequalities and quantum communication complexity. *Phys. Rev. Lett.* **92**, 127901 (2004).
- Pawłowski, M. & Żukowski, M. Entanglement-assisted random access codes. *Phys. Rev. A* **81**, 042326 (2010).
- Tavakoli, A. & Żukowski, M. Higher-dimensional communication complexity problems: classical protocols versus quantum ones based on bell's theorem or prepare-transmit-measure schemes. *Phys. Rev. A* **95**, 042305 (2017).
- Junge, M., Palazuelos, C. & Villanueva, I. Classical versus quantum communication in XOR games. *Quantum Inf. Process.* **17**, 117 (2018).
- Nielsen, M. A. & Chuang, I. *Quantum computation and quantum information* (Cambridge University Press, 2002).
- Muhammad, S. et al. Quantum bidding in bridge. *Phys. Rev. X* **4**, 021047 (2014).
- Zhang, J. et al. Experimental quantum "guess my number" protocol using multiphoton entanglement. *Phys. Rev. A* **75**, 022302 (2007).
- Martínez, D. et al. High-dimensional quantum communication complexity beyond strategies based on bell's theorem. *Phys. Rev. Lett.* **121**, 150504 (2018).
- Wei, K. et al. Experimental quantum switching for exponentially superior quantum communication complexity. *Phys. Rev. Lett.* **122**, 120504 (2019).
- Yao, A. C.-C. Quantum circuit complexity. In *Proc. 1993 IEEE 34th Annual Foundations of Computer Science*, 352–361 (IEEE, 1993).
- Raz, R. Exponential separation of quantum and classical communication complexity. In *Proc. thirty-first annual ACM symposium on Theory of computing*, 358–367 (ACM, 1999).
- Buhrman, H., Cleve, R. & Wigderson, A. Quantum vs. classical communication and computation. In *Proc. thirtieth annual ACM symposium on Theory of computing*, 63–68 (ACM, 1998).
- Bar-Yossef, Z., Jayram, T. S. & Kerenidis, I. Exponential separation of quantum and classical one-way communication complexity. In *Proc. thirty-sixth annual ACM symposium on Theory of computing*, 128–137 (Association for Computing Machinery, 2004).
- Horn, R. T., Babichev, S., Marzlin, K.-P., Lvovsky, A. & Sanders, B. C. Single-qubit optical quantum fingerprinting. *Phys. Rev. Lett.* **95**, 150502 (2005).
- Du, J. et al. Experimental quantum multimeter and one-qubit fingerprinting. *Phys. Rev. A* **74**, 042319 (2006).
- Smania, M., Elhassan, A. M., Tavakoli, A. & Bourennane, M. Experimental quantum multiparty communication protocols. *npj Quant. Inf.* **2**, 1 (2016).
- Moreno, G., Nery, R., de Gois, C., Rabelo, R. & Chaves, R. Semi-device-independent certification of entanglement in superdense coding. *Phys. Rev. A* **103**, 022426 (2021).
- Tavakoli, A., Pauwels, J., Woodhead, E. & Pironio, S. Correlations in entanglement-assisted prepare-and-measure scenarios. *arXiv* <https://arxiv.org/abs/2103.10748> (2021).
- Pauwels, J., Tavakoli, A., Woodhead, E. & Pironio, S. Entanglement in prepare-and-measure scenarios: many questions, a few answers. *arXiv* <https://arxiv.org/abs/2108.00442> (2021).
- Brunner, N., Cavalcanti, D., Pironio, S., Scarani, V. & Wehner, S. Bell nonlocality. *Rev. Mod. Phys.* **86**, 419 (2014).
- Buhrman, H. et al. Quantum communication complexity advantage implies violation of a bell inequality. *Proc. Natl Acad. Sci. USA* **113**, 3191 (2016).
- Van Dam, W. Implausible consequences of superstrong nonlocality. *Nat. Comput.* **12**, 9 (2013).
- Brassard, G. et al. Limit on nonlocality in any world in which communication complexity is not trivial. *Phys. Rev. Lett.* **96**, 250401 (2006).
- Shutty, N., Wootters, M. & Hayden, P. Tight limits on nonlocality from nontrivial communication complexity; aka reliable computation with asymmetric gate

- noise. In *IEEE 61st Annual Symposium on Foundations of Computer Science (FOCS)*, 206–217 (IEEE, 2020).
40. Svetlichny, G. Distinguishing three-body from two-body nonseparability by a bell-type inequality. *Phys. Rev. D* **35**, 3066 (1987).
 41. Chaves, R., Cavalcanti, D. & Aolita, L. Causal hierarchy of multipartite Bell non-locality. *Quantum* **1**, 23 (2017).
 42. Jones, N. S., Linden, N. & Massar, S. Extent of multipartite quantum nonlocality. *Phys. Rev. A* **71**, 042329 (2005).
 43. Bancal, J.-D., Brunner, N., Gisin, N. & Liang, Y.-C. Detecting genuine multipartite quantum nonlocality: a simple approach and generalization to arbitrary dimensions. *Phys. Rev. Lett.* **106**, 020405 (2011).
 44. Brask, J. B. & Chaves, R. Bell scenarios with communication. *J. Phys. A Math. Theor.* **50**, 094001 (2017).
 45. Bell, J. S. On the einstein podolsky rosen paradox. *Phys. Phys. Fiz.* **1**, 195 (1964).
 46. Collins, D., Gisin, N., Popescu, S., Roberts, D. & Scarani, V. Bell-type inequalities to detect true n-body nonseparability. *Phys. Rev. Lett.* **88**, 170405 (2002).
 47. Bancal, J.-D., Branciard, C., Gisin, N. & Pironio, S. Quantifying multipartite non-locality. *Phys. Rev. Lett.* **103**, 090503 (2009).
 48. Chaves, R. et al. Quantum violation of an instrumental test. *Nat. Phys.* **14**, 291 (2018).
 49. Almeida, M. L. et al. Guess your neighbor's input: a multipartite nonlocal game with no quantum advantage. *Phys. Rev. Lett.* **104**, 230404 (2010).
 50. Navascués, M., Pironio, S. & Acín, A. Bounding the set of quantum correlations. *Phys. Rev. Lett.* **98**, 010401 (2007).
 51. Kelsey, J. et al. A reference for randomness beacons: Format and protocol version 2. No. NIST Internal or Interagency Report (NISTIR) 8213 (Draft). (National Institute of Standards and Technology, 2019).
 52. Renou, M.-O. et al. Genuine quantum nonlocality in the triangle network. *Phys. Rev. Lett.* **123**, 140401 (2019).
 53. Moroder, T., Bancal, J.-D., Liang, Y.-C., Hofmann, M. & Gühne, O. Device-independent entanglement quantification and related applications. *Phys. Rev. Lett.* **111**, 030501 (2013).
 54. Moreno, M. G. M., Brito, S., Nery, R. V. & Chaves, R. Device-independent secret sharing and a stronger form of bell nonlocality. *Phys. Rev. A* **101**, 052339 (2020).
 55. Moreno, G., Nery, R., Palhares, A. & Chaves, R. Multistage games and bell scenarios with communication. *Phys. Rev. A* **102**, 042412 (2020).
 56. Tavakoli, A., Żukowski, M. & Brukner, Č. Does violation of a Bell inequality always imply quantum advantage in a communication complexity problem? *Quantum* **4**, 316 (2020).
 57. Graffitti, F., Kundys, D., Reid, D. T., Brańczyk, A. M. & Fedrizzi, A. Pure down-conversion photons through sub-coherence-length domain engineering. *Quantum Sci. Technol.* **2**, 035001 (2017).
 58. Pickston, A. et al. Optimised domain-engineered crystals for pure telecom photon sources. *Opt. Express* **29**, 6991 (2021).
 59. Proietti, M. et al. Enhanced multiqubit phase estimation in noisy environments by local encoding. *Phys. Rev. Lett.* **123**, 180503 (2019).

ACKNOWLEDGEMENTS

We acknowledge the John Templeton Foundation via the Grant Q-CAUSAL No. 61084, the Serapilheira Institute (Grant No. Serra-1708-15763), the Brazilian National

Council for Scientific and Technological Development (CNPq) via the National Institute for Science and Technology on Quantum Information (INCT-IQ), Grants Nos. 307295/2020-6 and 406574/2018-9, the Brazilian agencies MCTIC and MEC, the São Paulo Research Foundation FAPESP (Grant No. 2018/07258-7). This work was supported by the UK Engineering and Physical Sciences Research Council (Grant Nos. EP/N002962/1 and EP/T001011/1). F.G. acknowledges studentship funding from EPSRC under Grant No. EP/L015110/1.

AUTHOR CONTRIBUTIONS

R.C., A.F., and M.P. conceived the project. G.M., S.B., R.N., R.R., and R.C. developed the theoretical framework. J.H., F.G., A.P., and C.M. performed the experiment and collected the data. J.H. and F.G. analysed experimental data and prepared figures. All authors contributed to writing the manuscript.

COMPETING INTERESTS

The authors declare no competing interests.

ADDITIONAL INFORMATION

Supplementary information The online version contains supplementary material available at <https://doi.org/10.1038/s41534-022-00520-8>.

Correspondence and requests for materials should be addressed to Rafael Chaves.

Reprints and permission information is available at <http://www.nature.com/reprints>

Publisher's note Springer Nature remains neutral with regard to jurisdictional claims in published maps and institutional affiliations.



Open Access This article is licensed under a Creative Commons Attribution 4.0 International License, which permits use, sharing, adaptation, distribution and reproduction in any medium or format, as long as you give appropriate credit to the original author(s) and the source, provide a link to the Creative Commons license, and indicate if changes were made. The images or other third party material in this article are included in the article's Creative Commons license, unless indicated otherwise in a credit line to the material. If material is not included in the article's Creative Commons license and your intended use is not permitted by statutory regulation or exceeds the permitted use, you will need to obtain permission directly from the copyright holder. To view a copy of this license, visit <http://creativecommons.org/licenses/by/4.0/>.

© The Author(s) 2022